Journal Name

ARTICLE TYPE

Cite this: DOI: 00.0000/xxxxxxxxxx

Collect of nectar by bumblebees: How physics of fluid demonstrates the prominent role of tongue's morphology

Amandine Lechantre,[a] Denis Michez,[b] and Pascal Damman*[a]

Received Date
Accepted Date

DOI: 00.0000/xxxxxxxxxx

Bumblebees and some other tiny animals feed from nectar by visiting flowers in their neighborhood. Some bees species appear to be highly specialized, their tongue being adapted to specific flowers. *Bombus terrestris* in contrast is able to feed on a wide variety of flowers and can thus be considered as a kind of universal nectar catcher. Since plant nectars show highly variable sugar content, *Bombus terrestris* have developed a capture mechanism that works for almost any fluid viscosity. Their tongues are decorated with very elongated papillae forming a hairy coating surrounding a rod-like main stalk. When settled on a flower, Bombus rapidly dip their tongue in the inflorescence to catch the highly sought-after nectar. To determine the physical mechanism at the origin of this outstanding ability, the capture dynamics was followed from videos recorded during viscous fluids ingestion. Surprisingly, the volume per lap and the lapping frequency are independent of the fluid viscosity over three orders of magnitude. To explain this observation, we designed a physical model of viscous dipping with structured rods. Predictions of the model compared to observations for bees showed that the nectar is not captured with the help of viscous drag, as proposed in the Landau-Levich-Derjaguin model, but thanks to the hairy structure that traps viscous fluid, capillary forces drastically limiting the drainage. Our approach can be transposed to others nectar foragers such as bats and hummingbirds.

1 Introduction

During evolution, various and sometimes surprising methods have been developed by animals to ingest liquids. A compendium of drinking strategies encountered in animal realm is compiled in the review of Kim and Bush[1]. They emphasize that animals adapt their method to their size and the properties of the fluid to be ingested. Gravity, viscous, capillary, and inertial forces thus balance to determine the rate and volume of captured fluid. For most insects and other tiny animals, beyond the action of muscles, capillary and viscous forces are dominant. Interestingly, viscous forces both facilitate fluid capture (*e.g.*, drag in viscous dipping) or hinder it (*e.g.*, dissipation in capillary filling of tubes). While viscosity of water is relatively low, plant secretion like nectar can show high viscosity challenging the food intake strategy of the floral visitors (*e.g.*, bees visit flowers producing nectar from 0.001 to 0.5 Pa.s)[2–4]. In addition, the viscosity of plant secretions can exhibit large variations during the same day, depending on weather conditions. The collect of nectar can be seen as a simple energy supply taking advantage of the high sugar fraction contained in these plant secretions. Its optimization should maximise the energy-intake rate $\dot{E}$ defined by the product of the energy content per unit mass of the sugar, ε, the density ρ of the nectar, the volumetric fraction of sugar in nectar C and the volumetric flow rate Q through the relation $\dot{E} = \varepsilon\rho CQ$.[5] While ε and ρ can be considered as constants (small variations related to chemical composition and concentration can however be observed even within the same flower species), C and Q strongly depend on the viscosity of the nectar. This viscosity exponentially increases with the sugar concentration at a given temperature and also depends on the exact composition of the nectar (the ratio of the different types of sugar contained in the nectar but also the presence of various compounds such as amino acids or enzymes)[3]. To optimize $\dot{E}$, animals should then both maximize the sugar content C and the flow rate Q. The sugar content C is determined by the type of visited flowers, a tremendously relevant parameter but completely fixed by the characteristics of the foraging area. From the physical point of view, the only adjustable parameter is Q. This important parameter could be adapted through both the shape and the kinematics of the tongue. Careful analysis of these relationships could ultimately give a strong support to the idea that evolution has selected the species optimizing the capture of

[a] *Laboratoire Interfaces & Fluides Complexes, Université de Mons, 20 Place du Parc, B-7000 Mons, Belgium; E-mail: pascal.damman@umons.ac.be*
[b] *Institut des Biosciences, Laboratoire de Zoologie, Université de Mons, 20, Place du parc, 7000 Mons, Belgium.*

nectar in a given region and/or a given group of plants.

Kim *et al.* propose two main mechanisms to describe the capture of nectar by various animals, including bees, hummingbirds, butterflies, bats. The first one is related to suction through the action of capillary forces or muscles, the second one being based on viscous dipping [1,6]. To theoretically estimate the evolution of ingestion rates with nectar viscosities, they proposed a reasonable hypothesis: the animals capture the fluid with a constant power. This assumption yields scaling laws for the flow rates (*i.e.*, $Q \propto \eta^{-1/2}$ for suction and $Q \propto \eta^{-1/6}$ for viscous dipping, η being the nectar viscosity), that qualitatively fit the compiled experimental data found in the literature [6]. It should be noted however that the leading hypothesis of constant retraction power is not supported by any experimental observations in the literature. Last but not least, they assimilated animals' tongues to simple tubes or smooth rods, the micro-structures such as hairy papillae, that decorate the tongues of bees and bats, being discarded. More recent works suggest however that the capture of nectar depends on the morphology and the dynamic of the tongue. Yan et al. proposed a mechanism of capture based on a very complex coordinated dynamics between the back and forth movement of the tongue in the fluid coupled to the erection of the hairy papillae coating the tongue [7–12]. In summary, while several works in the literature discuss the capture of nectar by bees, the true influence of the micro-structures of the tongue is still questioned and a physical model describing quantitatively the fluid capture by nectarivores remains to be designed.

In this paper, we will address these specific problems by studying in details the collect of nectars by a single species, *Bombus terrestris*. The studied species has been chosen for its polylectic character, i.e., bees that collect nectar and pollen from the flowers of a variety of unrelated plants [13]. The advantage of focusing the study on a non-specialized species is to avoid exotic tongue morphologies resulting from a specific co-evolution of flowers and bees [14]. Our study is based on the analysis of videos of bumblebees ingesting nectars of various viscosities and a detailed physical study of the viscous dipping for smooth and structured rods. The quantitative comparison of biological data with predictions of the physical model should help to derive a novel perspective about nectar capture.

2 Experimental Section

Bumblebees

We study *Bombus terrestris audax*. The worker bumblebees come from a colony bought to *Biobest firm* (Westerlo, Belgium). The colony was kept at the temperature of 27°C and humidity of 65-70% [15]. They were fed every two days with pollen candies and a sweet solution imitating the nectar (Biogluc pink ®) is provided to them *ad libitum*.

Video recording of nectar capture

The experimental setup for observing the drinking process is based on a previously reported protocol [16]: before beginning the observation of the drinking process, bumblebees were starved at the room temperature in the dark from 2 to 4 hours. Then, the bumblebee is transferred into the holding tube which is a centrifuge tube of 15 mL with a 4 mm hole at the tip (Figure 1B). After a habituation phase of 3 minutes, the extension of the proboscis is motivated by presenting a drop of a solution of diluted honey. Finally, a capillary tube within a sweet solution of known viscosity (from 10^{-3} to 0.3 Pa.s) is presented to the bumblebee. The experiments are filmed by a camera Logitech C920, up to 30 frames per second.

Table 1 Dimensions of the structures. R_i, d, D and H represent the inner diameter of the rod, the width of a pillar, the gap between pillars and the depth of the microstructure, respectively. All lengths are given in mm.

Name	R_i	D	H	d
A	4.82	1.2	1.2	1.2
B	4.82	1.6	1.2	1.2
C	4.82	2.4	1.2	1.2
D	4.82	1.2	1.6	1.2
E	4.82	1.2	2.4	1.2
F	4.82	1.2	4.8	1.2
G	4.82	1.2	1.2	1.6
H	4.82	1.2	1.2	2.0
I	4.82	1.2	1.2	2.4

Physical model of the viscous dipping process

During experiments performed on smooth rods of diameter d (1 mm $< d <$ 6.9 mm) and on structured rods, the thickness of dragged fluid was followed over time via the measurement of the total mass of the fluid entrained on the rod. Fluids (silicon oil) of viscosity, η, of 0.5, 1 and 5 Pa.s were tested with withdrawal rates between 1 and 40 mm/s. The structured rods have been made by 3D printing via the company *Sculpteo*. The intern diameter, R_i, the gap between pillars, D, depth of the structure, H, and thickness of a ridge, d, of the different structures are compiled in the Table 1.

3 Results and discussion

Dynamics of nectar capture

To validate a physical model relating the nectar flow rate to the bumblebee's tongue characteristics, we need relevant values of ingestion rates Q, determining the energy-intake rates. For this purpose, we recorded videos of bumblebees (*Bombus terrestris*) capturing artificial nectars of different sugar content, *i.e.*, different viscosities (see Experimental Section for details). The fluid is contained in a capillary tube of 1mm diameter (Figure 1B). The evolution of the meniscus with time (Figure 1C) reveals small periodic variations related to the periodic movement of the tongue. After a short adaptation time, the curves become very regular, both in time and volume (with deviations less than 20%). Analysis of the meniscus displacement yields the average lapping rate ν and the average captured volume for each lap v_0 for different nectar viscosities spanning three orders of magnitude (Figure 1D). From these data, the ingestion rate $Q \sim \nu\, v_0$ can be computed. Counterintuitively, the ingestion rate does not depend upon the fluid viscosity (Figure 1E). The velocity of the tongue and the ingestion rate are thus not determined by the viscosity. These ob-

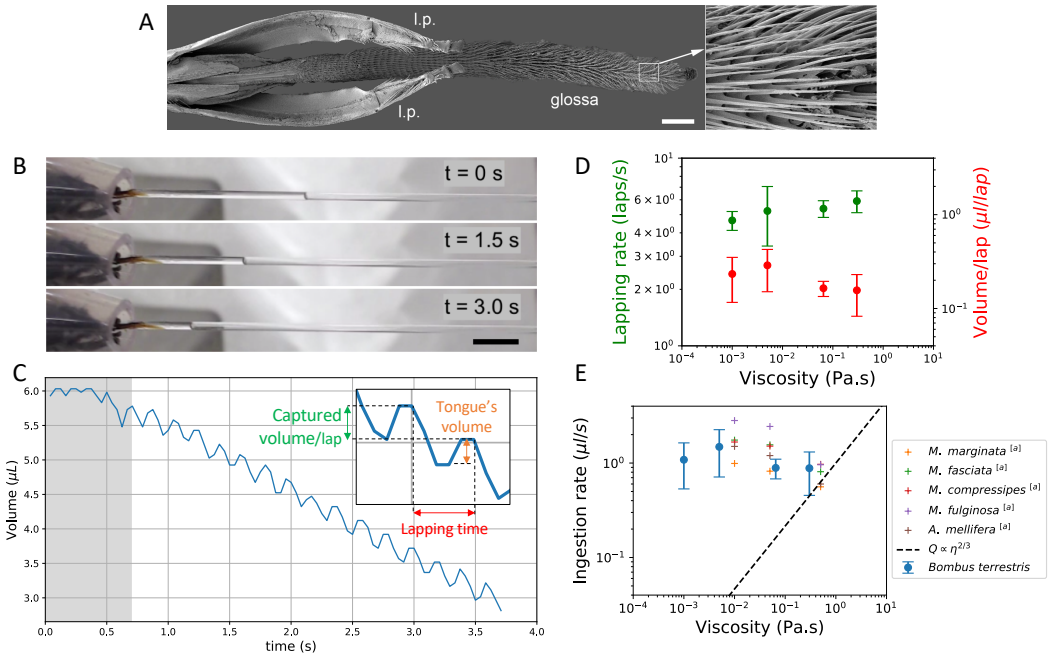

Fig. 1 A. Glossa and labial palpae (l.p.) of *Bombus terrestris* with a detail of the setae structure (scale bar: 400μm). B. Time sequence images of the collect of nectar by a bumblebee. The bumblebee is maintained in an opened holding tube placed close to a capillary tube of 1mm diameter containing the sugary solution. The evolution of the position of the meniscus on the capillary tube allows us to determine the quantity of captured solution (scale bar: 5 mm). C. Evolution of the volume of the solution with time in the capillary tube. The inset shows a close-up of the same graph. D. Lapping rate (in green) and captured volume by lap (in red) for different fluid viscosities (4 to 7 different bees for each viscosity). E. Ingestion rate for different viscosities. Our measurements correspond to the blue dots. Data from the literature appears as crosses[4]. The dashed black line represents the evolution of the ingestion rate following the LLD law calculated with a constant lapping rate.

servations contradict the constant power output hypothesis at the basis of the first proposed model[6], with $Q \propto \eta^{-1/6}$. These authors consider that, whatever the viscosity, the work per unit time required to overcome the viscous friction, or equivalently the power output is constant. For clarity, we briefly recall the main process of the previous analysis. The muscular power required to overcome the viscous drag should be given by $\dot{W} \sim \eta V^2 L$, where V and L are respectively the velocity and the length of the tongue.Considering a constant power output imposes that the lapping rate decreases with the viscosity according a $\nu \sim V/L \propto \eta^{-1/2}$ power law[6]. Instead, our experiments show that the lapping rate is found to be constant for a very large range of viscosities. It should be noted that our data are in close agreement with those previously reported in the literature[4].

The logical consequence of this observation is rather unexpected. It clearly indicates that, during a short period of adaptation lasting less than 1s (the grey zone in Figure 1C), the bumblebees are able to adjust the retraction force to the viscosity of the nectar. Such an adaptative behavior is supported by a previous study showing that bees prefer warmer and less viscous nectar, regardless of sugar concentration[17]. Hummingbirds have a sweet taste perception[18] but this observation suggests that bumblebees have a viscosity perception. Moreover high learning abilities have already been prove for honey bees and bumblebees[19,20]. This raises a fundamental question: What does determine the lapping frequency if it is not the muscle power ? We could only suggest hypothesis. For instance, limiting the captured nectar volume below the maximum amount they can swallow is an issue of survival[21].

As a first try, we amended the model previously proposed by Kim et al.[6] by replacing the constant power assumption by the observed constant lapping rate. As they suggested, the volume of nectar per lap can be estimated by considering a Landau-Levich-Derjaguin, LLD, mechanism[22,23]. The thickness of fluid dragged during the retraction is determined by the bees tongue radius R and the capillary number, $Ca = (\eta V/\gamma)$ through the relation $h \sim RCa^{2/3} \sim R(\eta V/\gamma)^{2/3}$, which suggests that the ingestion rate follows $Q \sim RhV \propto \eta^{2/3}$. As shown in Figure 1E, this law is in complete contradiction with the observed constant volume per lap, lapping rate and ingestion rate. Neither the independence with the viscosity nor the absolute values of Q, much higher than the predictions, are compatible with this model.

How could we thus explain the constant volume per lap for viscosities spanning three orders of magnitude ? The severe inconsistency of the previous model clearly suggests that we should discard the proposed LLD hypothesis and test other processes. In the following, we build a physical model of viscous dipping taking into account the influence of the micro-structures that decorate the bumblebees' tongue (Figure 1A).

Viscous dipping with micro-structured rods

Considering the shape of the tongue (*i.e.*, a stalk coated with sub-millimetric hairy papillae), the collect of nectar by bumblebees can be mimicked as the dipping of thin rods decorated with

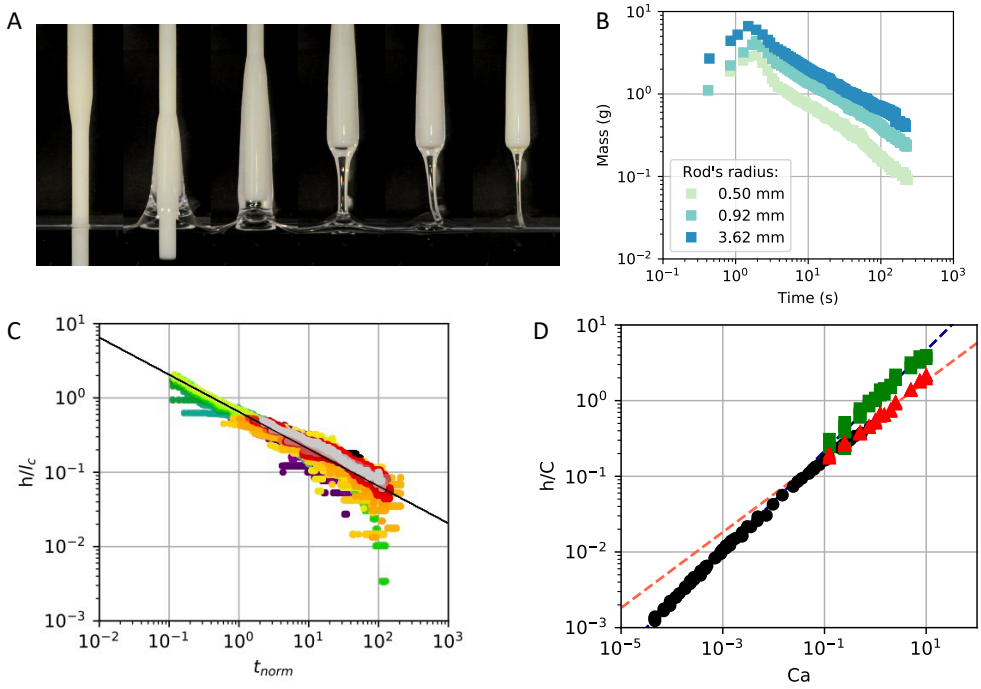

Fig. 2 A. Images sequence recorded during the withdrawal of a smooth rod (R = 2.41 mm, η = 5 Pa.s and V = 40 mm/s). B. Evolution of the mass of dragged fluid over time. C. Time evolution of the normalized thickness of dragged fluid during the drainage stage (normalized time $t_{norm} = (t\gamma/L\eta)$ where γ, L and η are respectively the surface tension, the immersed length and the fluid viscosity). The solid line represents a $t^{-1/2}$ power law. D. Evolution of the normalized maximal thickness of collected fluid with the capillary number, Ca (C is equal to l_c/R for thick/thin rods). Green squares: thin rods ($R < l_c$); Red triangles: Thick rods ($R > l_c$) and Black circles: previously reported data for plates[29,30]. The red and blue dashed line represent respectively a slope of 2/3 and 1/2.

regular micro-structures in a fluid of controlled viscosity. A few works were devoted to the influence of micro-structures on the viscous dipping with plates[24–26]. From the study of sanded glass plates, Krechetnikov *et al.* showed that, depending on the roughness σ_R and the thickness of the film of fluid h, three regimes can be defined: i) for $\sigma_R \ll h$, the roughness does not produce any observable effect and can be neglected, ii) For $\sigma_R \gg h$, the liquid essentially fill the cavities, the fluid thickness becomes independent of Ca (drag becomes negligible), and iii) the intermediate regime, $\sigma_R \sim h$, where both contributions are comparable. The fluid flow at the rough interface is perturbed and can be described by considering a slippage length at the solid-fluid interface[24]. Seiwert et al. extensively studied viscous dipping with silicon wafers decorated with regular arrays of micrometric pillars[25]. They also observed the three regimes first proposed by Krechetnikov, and suggest a model with two viscosities. In fact, the flow within the forest of pillars, that could be related to a wicking of the micro-structure, is replaced in the model by a layer of very large viscosity. They suggest that it is possible to consider separately the contributions from the roughness and from the drag, $h(Ca) = h_0 + h_{drag}(Ca)$. More recently, Nasto et al. reported the viscous dipping of plates coated with regular arrays of millimetric pillars. They showed that, for the studied range of experimental parameters, the final amount of dragged fluid is essentially determined by the drainage dynamics of the fluid trapped in the microstructure during the retraction time[26].

Unfortunately, none of these studies investigate experimental conditions close to these estimated for the capture of nectars by bumblebees, *i.e.*, large capillary numbers, $0.01 < Ca < 1$ and a rod-like geometry with submillimetric decorations[3,4]. Studies reported by Krechetnikov et al.[24] and Seiwert et al.[25] focused on plates and very small capillary numbers, $Ca < 10^{-2}$. Nasto et al. described the drainage of plates coated with large millimetric pillars[26]. The micro-structures on the tongue of *Bombus terrestris* are only spaced by 20 μm (Figure 1A), much smaller than the capillary length. In this case, capillary forces prevent any fluid drainage from the structure. We thus investigate viscous dipping with structures trying to mimic bee's tongues. Unfortunately, the hairy structure formed by an array of very elongated papillae is very difficult to produce by 3D printing. Instead we chose to use simpler shapes, reminiscent of honey spoons, *i.e.*, rods of finite length, different radius and decorated with periodic structure of valleys and ridges, keeping a radial symmetry. At first sight, these micro-structured rods seem to be far from the hairy structures observed for bumblebees but they appear to be helpful to derive the general rules governing capture of fluid with rods of complex shape.

Smooth rods. First, we study the fluid capture with smooth rods to investigate the influence of the radius. As shown in Figure 2 A and B, the withdrawal of a rod immersed in a viscous fluid involves the drag of fluid immediately followed by a drainage process. For ease of comparison with the theory, the measured mass of fluid is converted into a thickness, through the relation $M \sim \rho RhL$ with R the radius of the rod and L the immersed dis-

tance. As previously shown, the dynamics of drainage is determined by a balance of gravity, *i.e.*, the driving force, with a dissipative force dominated by the viscous flow in the dragged fluid layer. As shown in Figure 2C, it is adequately described by the scaling relation, $h/l_c \sim (\eta L/\gamma)^{1/2}\, t^{-1/2}$, (with the capillary length $l_c = (\gamma/\rho g)^{1/2}$), obtained by considering volume conservation and the Stokes equation[27,28].

When considering the collect of fluid by animals, the most relevant parameter is the maximum amount of nectar that could be obtained per lap. In Figure 2D, the maximum fluid thickness computed from the mass at maximum is plotted versus the capillary number for various radii. The data reported by Seiwert et al.[29] and Maleki et al.[30] for the viscous dipping of plates at low capillary numbers ($Ca < 0.1$) were added for clarity. For plates, previous studies showed that the evolution of fluid thickness with Ca can be described by two asymptotic regimes. At low Ca, the LLD relationship $h \sim l_c Ca^{2/3}$ fully determines the thickness[22]. Above a critical capillary number Ca^*, a transition towards a gravity dominated regime characterized by the relation $h \propto Ca^{1/2}$ is observed[23]. For rods, the situation is slightly more complex. At low Ca, all data for plates and rods collapse on a single master curve. For high Ca however, the fluid thicknesses measured for various rods collapse on two different curves, depending on their radius. For thin rods, $R < l_c$, the fluid thickness follows the classical $h \propto Ca^{2/3}$ LLD relationship. For thick rods, $R > l_c$, the rods behave in the same way as plates, with a transition towards a gravity dominated regime with $h \propto Ca^{1/2}$. The occurence of two regimes for the same range of Ca can be rationalized by considering a change of the relevant length-scale, l_c vs R. Thick rods, $R > l_c$, can be considered as plates. We should thus have to explain: i) the transition from capillary to gravity dominated regimes observed for plates and thick rods, and ii) the disappearance of this transition for thin rods.

The transition between two asymptotic behaviors at a critical capillary number was previously reported for plates[23], and corresponds to a switch from a Laplace pressure dominated to a hydrostatic dominated regimes. The difference in dynamics results from a change in the pressure gradient term in the Stokes equation, $\eta \nabla^2 V = \nabla P$. In the capillary regime, $\nabla P \sim \gamma\kappa/\ell$, where κ, ℓ are the curvature of the static meniscus and the length of the dynamic meniscus. The assumption that dynamic curvature should be equal to the static one, $\kappa \sim 1/l_c \sim h/\ell^2$, finally gives the LLD relationship $h \sim l_c Ca^{2/3}$. In the gravity dominated regime, also called Derjaguin regime[31], $\nabla P \sim \rho g$ which immediately gives the relation $h \sim l_c Ca^{1/2}$. The gravity regime appears when $\rho g \ell > \gamma/l_c$, *i.e.* when $Ca > 1$ in agreement with our observations for thick rods (Figure 2D).

The disappearance of the transition for thin rods can also be rationalized from the derivation of the LLD model. For rods, there are two limiting cases for defining the mean curvature : i) $\kappa \simeq 1/R$ which yields the relation $h \sim RCa^{2/3}$, this corresponds to the rod-like regime; or ii) $\kappa \simeq 1/l_c$, giving the relation $h \sim l_c Ca^{2/3}$, we name this regime plate-like. The transition between these two-regimes corresponds to $R \simeq l_c$. For thin rods, the $Ca^{1/2}$ gravity regime only appears when $\rho g \ell > \gamma/R$. This condition requires that $Ca > Ca^* \sim (l_c/R)^6$. In most cases, this condition cannot be fulfilled and this regime is not observed (for instance, it should appear for $Ca > 200$ for the thin rods used here).

Structured rods. For studying the influence of the micro-structure, we used thick rods corresponding to the visco-gravitational regime, $h \propto Ca^{1/2}$. While keeping a radial symmetry, various sizes of micro-structures were used, they are summarized in Table 1. The most obvious difference observed with structured rods with respect to their smooth counterparts appears during the drainage (Figure 3 B). The drainage dynamic does not follow anymore the $t^{-1/2}$ power law but instead asymptotically tends toward a constant value characterized by the size and geometry of the rod. This tendency can be related to the fluid trapped in the micro-structure by capillary forces that cannot be drained.

The presence of micro-structures on the rods raises several fundamental questions regarding the capture of viscous fluid. How to quantitatively analyse the viscous drag for such heterogeneous system ? How to define the thickness of dragged fluid ? What is the influence of valleys and ridges on viscous forces ?

Unfortunately, there is no obvious way to analyse the amount of fluid collected through viscous drag for such complex shapes. Nevertheless, to be consistent with the results obtained for smooth rods, we choose to convert the mass of fluid as an effective thickness, defined by the relation $M \sim \rho R_i L h_{eff}$, with R_i the internal radius of the structured rod and L the immersed distance. Interestingly, this effective thickness takes into account both the depth and density of ridges/valleys within a single parameters. The relevance of this particular choice will become clear later. The evolution of the effective thickness with the capillary number, Figure 3C, shows drastic deviations with respect to smooth rods. Instead of a master plot with all curves collapsing, well-separated curves are observed for the different structures. To rationalize these seemingly disparate curves, we follow the methodology previously reported[24,25] and estimate the thickness from two contributions : i) the first one is related to fluid trapped in the micro-structure, h_0; ii) the second contribution arises from the fluid carried away by the viscous drag, h_{drag}. As suggested by Kretchnikov[24], this procedure, consisting in compiling two asymptotic behaviors, is relevant considering the global evolution of the effective thickness with Ca. For small Ca, the viscous forces are negligible, only the fluid trapped in the structures is carried away and the thickness is independent of Ca. For large Ca, the viscous forces become so large that we can neglect the trapped fluid, the curves become closer to the $h/l_c \sim Ca^{1/2}$ law observed for smooth rods. The effective thickness of fluid wrapping the rod should then be given by, $h_{eff} = h_0 + h_{drag}$ where h_0 depends on the size and geometry of the micro-structure. To test this model, we measure h_0 from raw data by eliminating the dynamic part of the thickness, through the relation $h_0 = h_{eff} - l_c Ca^{1/2}$. As shown in Figure 3D, the measured trapped fluid thickness is in agreement with the h_0 estimated from the geometrical characteristics of the micro-structures, $h_{0theo} = h(d/(D+d))$. Conversely, the contribution related to viscous drag, h_{drag}, can be obtained from h_{eff} by subtracting the trapped fluid thickness, h_0. Figure 3E shows that the fluid carried away from the viscous forces for these structured rods follow quantitatively the same law than smooth rods, $h/l_c \sim Ca^{1/2}$. However, when approaching a critical capillary number, Ca_S^*, the

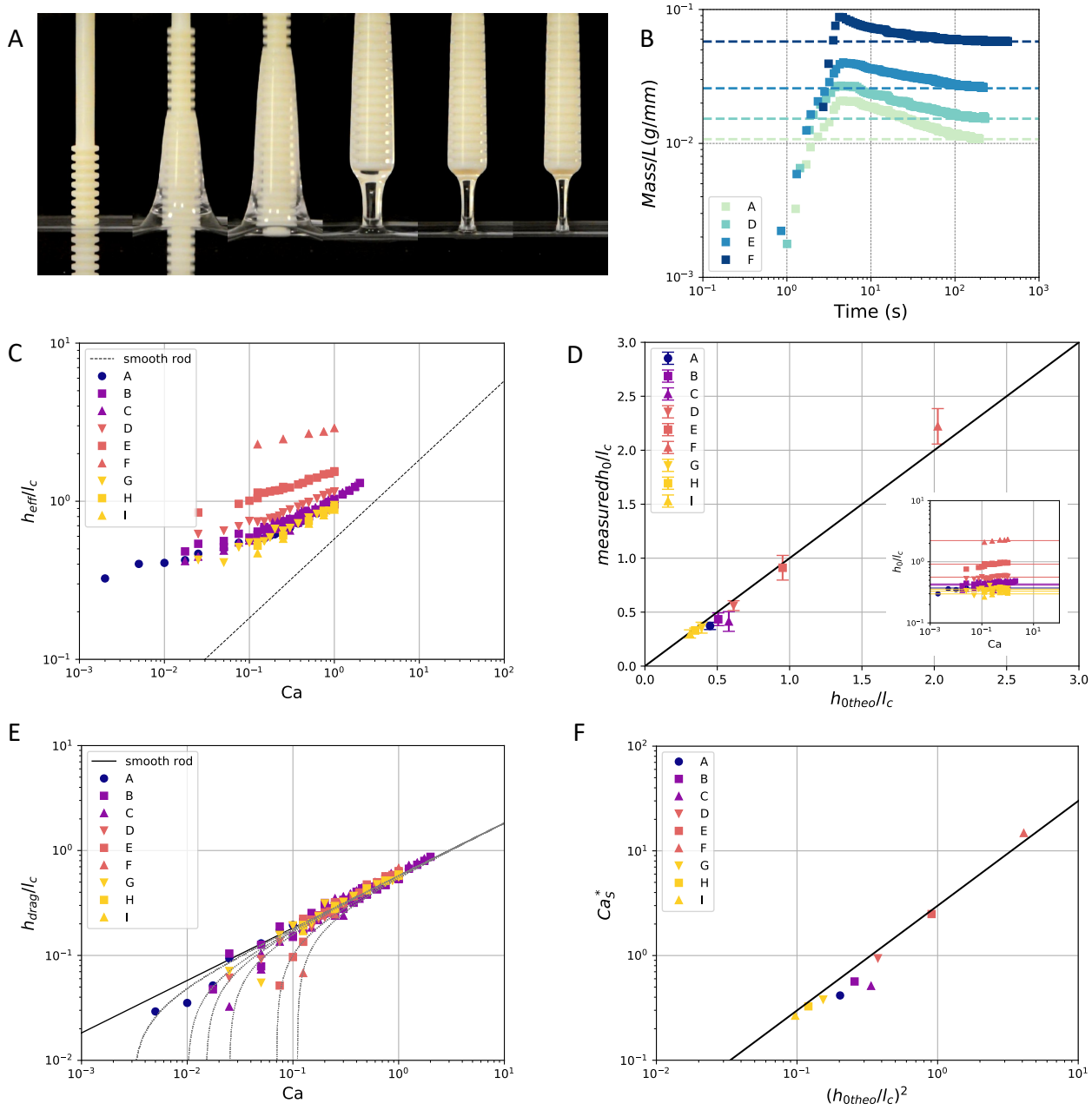

Fig. 3 A. Images sequence recorded during the withdrawal of a structured rod ('A' rod, R_i = 2.41 mm, h=d=D= 1.2 mm), η = 5 Pa.s and V = 40 mm/s). B. Time evolution for mass of captured fluid per immersed length unit. C. Evolution of the effective thickness of collected fluid with the capillary number. The dotted black line represents the data observed for smooth thick rods. D. Comparison of measured and calculated trapped fluid h_0. Inset: evolution of h_0 with Ca for the different structures. E. Plot of the dragged thickness contribution h_{drag} with the capillary number. Dotted lines represent theoretical predictions for structured rods. The solid line corresponds to smooth rods. F. Plot of the measured critical capillary number Ca_S^* versus the calculated value $(h_{0theo}/l_c)^2$ (see text).

contribution related to the viscous drag vanishes as illustrated by the drastic deviations observed at low Ca for the curves of Figure 3E. This critical capillary number Ca_S^* associated to the transition from trapped to viscous dominated regimes can be defined by considering that $h_0 = h_{drag}$, which yields $Ca_S^* \sim (h_0/l_c)^2$. The agreement between measured and calculated Ca_S^* gives an additional support to the proposed separation of contribution to describe the fluid drag of structured rods (Figure 3F). It should also be noted that there is no flow perturbations related to any interfacial slippage due to the structures detected in the measurements. Considering the previous studies[24,25,32], this can be explained by considering that i) in contrast to previous works on arrays of pillars, the fluid is here completely trapped in the structures (due to the "honey spoon" shape of the rods); ii) the observed fluid thicknesses are millimetric and probably larger than the slippage length.

Application of the model to bumblebees

The proposed physical model based on structured rods could be easily transposed to bumblebees to get the volume per lap ($v_0 \sim RLh$, with R, L the radius and length of the tongue). Figure 4 shows the evolution of the effective thickness of captured nectar with the capillary number. To apply the model to bumblebees, we should first determine the corresponding regime (gravitational vs capillary and trapped vs drag) by comparing the capillary numbers to the critical ones. Regarding the transition between capillarity and gravity dominated regimes, the tongue of the studied bumblebees corresponds to a thin rod, $R \simeq 0.1$mm, decorated with flexible papillae of length, $h_0 \simeq 0.15$mm. First, these data yields very large critical capillary number, $Ca^* \sim (l_c/R)^6 = 10^6$. Bumblebees thus always collect the nectar in the capillary dominated regime. Secondly, we have shown that a transition from trapped to viscous dominated regimes appears for a critical capillary number. Its expression must be adapted to the bumblebees' characteristics. Considering that $h_0 = h_{drag} \sim RCa^{2/3}$, we obtain $Ca_S^* \sim (h_0/R)^{3/2} \simeq 1.9$. The operating range of capillary numbers for bumblebees ranges between $10^{-2} < Ca < 0.1$, we could assume that the collected nectar is essentially located in the microstructure, the amount of nectar taken by the viscous drag being negligible. As shown in Figure 4, the predictions of the physical model is quantitatively in agreement with the values measured for living bumblebees without any fitting parameter. Finally, the trapping of the nectar within the papillae is only the first stage of the collect of nectar by bumblebees. Once the tongue is filled with nectar and retracts, the nectar is unloading in a tube formed by labial palpae (Figure 1A). The loaded tongue is squeeze by labial palpae acting like a wedge and the nectar is sucked into the mouth by action of the pharyngeal pump[33]. The collect of nectar for bumblebees can be viewed as a "mopping-squeezing" mechanism.

4 Conclusions

In conclusions, this study gives a new insight into the interaction of viscous fluid with structured solid objects. We have rationalized viscous dipping for unexplored experimental conditions, *i.e.*

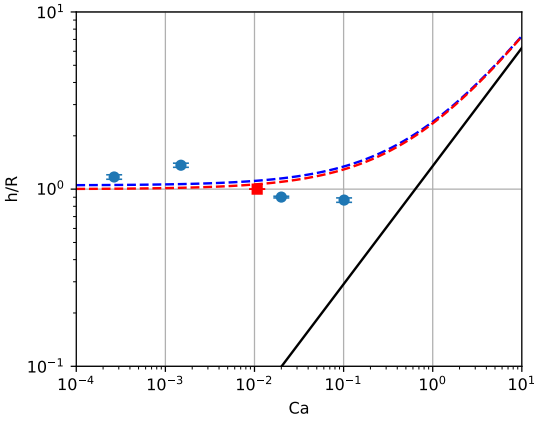

Fig. 4 Evolution of normalized thickness of nectar collected by bumblebees (blue circles) or bats (red circles, data reported in[34]) with the capillary number. The black solid line corresponds to the law expected for smooth rods ($R = 0.1$mm) and the dashed lines represent the predictions of the new model for bumblebees (blue) or bats (red).

millimetric rods decorated with micro-structures of radial symmetry. The assumption that it is safe to describe the dragged fluid with two independent contributions: one related to the fluid trapped in the micro-structure, and the other from the fluid carried away by the viscous drag, is validated from our experiments. Regarding the behavior of bumblebees, in contrast to previous studies, this quantitative work demonstrates that viscous dipping (dark line on the Figure 4) is not the dominant mechanism used by bumblebees to capture nectar. This clearly justifies the evolutionary purpose of the hairy micro-structure of papillae found at the tongue tip for many bees (Figure 1A). Finally, the proposed physical model could probably be adapted to other animal species. For instance, some bats also capture nectar by using erectile papillae forming a hairy structured tongue. As we can see in Figure 4, the predictions of the proposed model are compatible with the thickness of the dragged nectar measured for bats[34].

Conflicts of interest

There are no conflicts to declare.

Acknowledgements

A.L. and P.D. acknowledge T. Salez for highly valuable suggestions and careful reading of the manuscript, P. Rambach and D. Dumont for countless fruitful discussions. S. Cuvelier is acknowledged for his technical assistance. This work benefited from financial supports from the Fonds National de la Recherche Scientifique (PDR research project T.0109.16 "capture biomimétique de fluide" and CDR project J.0191.17 "Mimicking elasticity with viscous fluids") and from an Action de Recherche Concertée (UMONS, research project "Mecafood").

Notes and references

1 Kim W, Bush JWM (2012) Natural drinking strategies. *Journal of Fluid Mechanics* 705:7–25.

2 Percival MS (1961) Types of nectar in angiosperms. *The New Phytologist* 60(3):235–281.

3 Harder LD (1986) Effects of nectar concentration and flower

depth on flower handling efficiency of bumble bees. *Oecologia* 69:309–315.

4 Roubik DW, Buchmann SL (1984) Nectar selection by *Melipona* and *Apis mellifera* (hymenoptera: Apidae) and the ecology of nectar intake by bee colonies in a tropical forest. *Oecologia* 61(1):1–10.

5 Kingsolver JG, Daniel TL (1979) On the mechanics and energetics of nectar feeding in butterflies. *Journal of Theoretical Biology* 76(2):167–179.

6 Kim W, Gilet T, Bush JWM (2011) Optimal concentrations in nectar feeding. *PNAS* 108(40):16618–16621.

7 Yang H, Wu J, Yan S (2014) Effects of erectable glossal hairs on a honeybee's nectar-drinking strategy. *Applied Physics Letters* 104(263701):1–4.

8 Chen J, Wu J, Yan S (2015) Switchable wettability of the honeybee's tongue surface regulated by erectable glossal hairs. *Journal of Insect Science* 15:1–5.

9 Zhao C, Wu J, Yan S (2015) Observations and temporal model of a honeybee's hairy tongue in microfluid transport. *Journal of Applied Physics* 118(194701):1–7.

10 Wu J, Zhu R, Yan S, Yang Y (2015) Erection pattern and section-wise wettability of honeybee glossal hairs in nectar feeding. *Journal of Experimental Biology* 218:664–667.

11 Zhu R, Lv H, Liu T, Yang Y, Wu J, Yan S (2016) Feeding kinematics and nectar intake of the honey bee tongue. *Journal of Insect Behavior* 29:325–339.

12 Yang Y, Wu J, Zhu R, Li C, Yan S (2017) The honeybee's protrusible glossa is a compliant mechanism. *Journal of Bionic Engineering* 14:607–615.

13 Rasmont P, Coppée A, Michez D, De Meulemeester T (2008) An overview of the *Bombus terrestris* (l.1758) subspecies (hymenoptera: Apidae). *Annales de la Société Entomologique de France* 44:243–250.

14 Müller A (2006) Unusual host-plant of *Hoplitis pici*, a bee with hooked bristles on its mouthparts (hymenoptera: Megachilidae: Osmiini). *European Journal of Entomology* 103:497–500.

15 Velthuis HH, van Doorn A (2006) A century of advances in bumblebee domestication and the economic and environmental aspects of its commercialization for pollination. *Apidologie* 37:421–451.

16 Ma C, Kessler S, Simpson A, Wright G (2016) A novel behavioral assay to investigate gustatory responses of individual, freely-moving bumble bees (*Bombus terrestris*). *Journal of Visualized Experiments* 113:1–7.

17 Nicolson SW, de Veer L, Köhler A, Pirk CWW (2013) Honeybees prefer warmer nectar and less viscous nectar, regardless of sugar concentration. *Proceedings of the Royal Society* 280(20131597).

18 Baldwin MW, et al. (2014) Evolution of sweet taste perception in hummingbirds by transformation of the ancestral umami receptor. *Science* 345(6199):929–933.

19 Dukas R, Real LA (1993) Effects of nectar variance on learning by bumble bees. *Animal Behaviour* 45:37–41.

20 Sherry DF, Strang CG (2015) Contrasting styles in cognition and behaviour in bumblebees and honeybees. *Behavioural Processes* 117:59–69.

21 Fewell JH, Winston ML (1995) Regulation of nectar collection in relation to honey storage levels by honey bees, *Apis mellifera*. *Behavioral Ecology* 7(3):286–291.

22 Landau L, Levich B (1942) Dragging of a liquid by a moving plate. *Acta Physicochimimica URSS* 17(1-2):141–153.

23 de Ryck A, Quéré D (1998) Gravity and inertia effects in plate coating. *Journal of Colloid and Interface Science* 203:278–285.

24 Krechetnikov R, Homsy GM (2005) Experimental study of substrate roughness and surfactant effects on the landau-levich law. *Physics of Fluids* 17(102108).

25 Seiwert J, Clanet C, Quéré D (2011) Coating of a textured solid. *Journal of Fluid Mechanics* 669:55–63.

26 Nasto A, Brun PT, Hosoi AE (1998) Viscous entrainment on hairy surfaces. *Journal of Colloid and Interface Science* 203:278–285.

27 Herczynski A, Cernuschi C, Mahadevan L (2011) Painting with drops, jets, and sheets. *Physics Today* 64(6):31–36.

28 Jeffreys H (1930) The draining of a vertical plate. *Mathematical Proceedings of the Cambridge Philosophical Society* 26(02):204–205.

29 Seiwert J (2010) Ph.D. thesis (Ecole Polytechnique X).

30 Maleki M, Reyssat M, Restagno F, Quéré D, Clanet C (2011) Landau-levich menisci. *Journal of Colloid and Interface Science* 354:359–363.

31 Derjaguin BV (1993) On the thickness of the liquid film adhering to the walls of a vessel after emptying. *Progress in Surface Science* 43(1-4):134–137.

32 Rio E, Boulogne F (2017) Withdrawing a solid from a bath: How much liquid is coated? *Advances in Colloid and Interface Science* 247:100–114.

33 Krenn HW, Plant JD, Szucsich NU (2005) Mouthparts of flower-visiting insects. *Arthropod Structure & Development* 34:1–40.

34 Harper CJ, Swartz SM, Brainerd EL (2013) Specialized bat tongue is a hemodynamic nectar mop. *PNAS* 110(22):8852–8857.